Dynamics of Bent Molecules in Gels

Udayan Mohanty*,† and Clifford Henry Taubes‡

Department of Chemistry, Boston College, Chestnut Hill, Massachusetts 02467, and Department of Mathematics, Harvard University, Cambridge, Massachusetts 02138

Received: March 7, 2003

A quantitative predictive model of the electrophoretic mobility of a bent molecule of cylindrical symmetry relative to a straight one in gel is described. The force acting on the surface of the molecule is shown to be the minimum value of a variational functional of the fluid velocities whose minimizer satisfies the large viscosity solution of the incompressible Brinkman−Navier−Stokes equations. By exploiting the variational approach, our model readily predicts, in agreement with experimental data, that the electrophoretic mobility of the molecule bent at the middle is smaller than that of the same molecule with a bend at the end. We apply the methodology to describe the electrophoretic mobility of intrinsically bent DNA molecules in polyacrylamide gels. The predictions are compared with available experimental data as well as a semiempirical relation between the relative electrophoretic mobility and the bend angle by Thompson and Landy.

1. Introduction

Gel electrophoresis is an often used analytical technique in molecular biology. However, the mechanism underlying electrophoresis is poorly understood. This lack of understanding is demonstrated by the discovery that the molecular weight dependence of electrophoretic mobility of small single and double stranded nucleic acid fragments is anomalous.[1−4]

A predominantly held notion is that macromolecules much larger than its persistence length migrates in a gel by neptation, i.e., snake like movement[4−10] and that this mode of transport holds for nucleic acid fragments.[11−16] A computer simulation extension of reptation ideas capable of quantifying dynamics of polyelectrolyte molecules in gel was first implemented by Levene and Zimm.[11] These simulations show that the gel electrophoretic mobility of the molecule with a bend at the center is smaller than the mobility of the same molecule with a bend at the end.[11]

Current simulations and models have not been sufficiently developed so as to quantitatively describe gel retardation of bent molecules as well as bend-induced retardation of protein−nucleic complexes in gels.[18−32] Consequently, predictions of gel electrophoretic mobility of intrinsically curved nucleic fragments are based on a comparison of the mobility of the molecule with a bend at the center with that near its end, and relating this ratio to the mean squared end-to-end distance of the bend molecule.[13]

In this paper we provide a predictive model of why a cylindrically shaped molecule which incorporates a structural bend migrate more slowly in a gel than a straight rod-like molecule. The model predicts a quantitative correlation between the bend angle and the mobility. The organization of this paper is as follows. In section 2, we introduce a model for the dynamics of cylindrically shaped molecules, in gel. A variational formulation of the "force" per unit length that acts on the molecule is formulated in section 3. In section 4, the friction coefficient of an infinitely long cylindrically shaped molecule in a direction parallel and perpendicular to its symmetry axis is explicitly solved. The following section exploits the variational formulation of the "force" functional to place lower and upper bounds on the friction coefficient of a cylindrically shaped molecule of finite length. The generalization of this approach to a bent molecule is briefly discussed in section 6. In the next section, our methodology is utilized to describe the gel mobility of intrinsically curved DNA molecules. We compare the predictions of the model with experimental data and with other models. A critical assessment of the basic assumptions of the model as applied to nucleic acid is discussed in section 8.

2. Model

We assume that each molecule is cylindrically shaped of diameter a, occupies a volume C, and is moving through the gel with constant velocity v_o. The coordinate system is such that $-v_o$ is pointed along the positive z direction. In this model, the gel fibers of concentration ρ are regarded as stationary beads in the liquid of viscosity η. Each bead provides a point source of friction ζ. We define the hydrodynamic shielding length l of the gel by[33,34]

$$l^{-2} = \frac{\rho\zeta}{\eta} \tag{1}$$

l is a measure of the average spacing between the fibers. Let v represent the velocity of the liquid and P the ambient pressure. We then introduce relative velocity $u = v - v_o$ and scaled pressure $p = \eta P$. This done, our model uses the hydrodynamic equations

$$-\Delta u + l^{-2}u = \frac{\nabla p}{\eta} \tag{2}$$

$$\nabla\cdot u = 0 \tag{3}$$

together with the constraints that $u = (0,0,v_o)$ on the boundary, ∂C, of the volume C occupied by the molecule and $u \to 0$ as $|x| \to \infty$. Here, ∇ is the gradient operator and $\Delta = \nabla\cdot\nabla$ is the Laplacian.

* Corresponding author.
† Boston College.
‡ Harvard University.

10.1021/jp030309f CCC: $25.00
Published on Web 05/30/2003

Thus, the gel material is idealized as a collection of fixed sources of point friction for the water that moves through it. These fixed points have a given concentration. The cylindrical volume of the macromolecule is excluded to the solvent and provides boundary conditions for the water on its surface. All gel particles are also external to this excluded volume. We have ignored the elastic response of the gel, but the model, as will be shown, explicitly contains enough to provide a reasonable basis for a reduced macromolecular mobility; this allows us to sharply address the question of whether a bent cylinder has a lower mobility than a straight one.

3. Variational Formulation

The force per unit length, F, exerted by the liquid and the gel on the surface of the macromolecule is defined in terms of the force functional

$$f = v_o^{-2}\int_{\partial C}\int(-u_j(\partial_j u_k + \partial_k u_j + P\delta_{jk})n_k) \tag{4}$$

by setting $F = f\eta v_o$. In eq 4 and below, the indices correspond to the components of the indicated vectors with respect to a Cartesian coordinate system, $\{n_k\}$'s are the components of the unit vector, outward pointing normal vector to boundary, δ_{ij} is the Kronecker delta, and any repeated indices are summed.

On applying the divergence theorem to eq 4 and making use of eq 2, one can express the "force functional" per unit length as a volume integral

$$f = v_o^{-2}\int_{\Omega}\int\int(\partial_j u_k\partial_j u_k + \partial_j u_k\partial_k u_j + l^{-2}u_j u_j) \tag{5}$$

Here, Ω is the volume external to that occupied by the molecule. Now consider the quantity

$$\mathcal{F}(b) = \int_{\Omega}\int\int(\partial_j b_k\partial_j b_k + \partial_j b_k\partial_k b_j + l^{-2}b_j b_j) \tag{6}$$

where b is a test function on Ω that is well behaved as $|x| \to \infty$. We consider the collection $\mathcal{N}$ of test functions on Ω that equal (0,0,1) on the boundary, have zero divergence and vanish as $|x| \to \infty$. It turns out that there is a solution u to eq 2 such that $v_o^{-1}u$ is in the set $\mathcal{N}$, and that achieves the minimum of $\mathcal{F}$ on $\mathcal{N}$.[35]

4. Infinitely Long Cylindrical Molecule

In this section we explicitly calculate the parallel and the perpendicular components of the velocity as well as the frictional coefficient of an infinitely long cylindrical shaped molecule.

4.1. Velocity Field. The axis of the infinitely long cylindrical molecule passes through the origin and we choose the coordinate axis so that the central axis is parallel to the vector $(\sin\theta,0,-\cos\theta)$. We decompose the velocity vector $(0,0,v_o)$ into components that are parallel and orthogonal to the cylindrical axis

$$(0,0,v_o) = v_o\cos\theta\,(\sin\theta,0,\cos\theta) + v_o\cos\theta\,(-\cos\theta,0,\sin\theta) \tag{7}$$

Because eq 2 is linear, the solution can be expressed in terms of parallel $u_{||}$ and perpendicular $u_\perp$ components

$$u = (v_o\cos\theta)u_{||} + (v_o\sin\theta)u_\perp \tag{8}$$

The solution for the parallel component of the velocity, $u_{||}$, is

$$u_{||} = G(a)^{-1}G(\rho)(\sin\theta,0,\cos\theta) \tag{9}$$

where $\rho = ((x\cos\theta - z\sin\theta)^2 + y^2)^{1/2}$ and $G(s)$ is the fundamental solution to the modified Bessel equation

$$-G_{ss} - s^{-1}G_s + l^{-2}G = 0 \tag{10}$$

having $\ln(s)$ singularity as $s \to 0$ and decaying to zero as $s \to \infty$; here the subscripts with respect to s indicate partial derivatives.

The perpendicular component of the velocity is found to be

$$u_\perp = G(a)^{-1}G(\rho)(0,0,1) + G(a)^{-1}l^2T(\rho)(0,2yx'/\rho^2,(x'^2 - y^2)/\rho^2) \tag{11}$$

where $x' = x\cos(\theta) - z\sin(\theta)$ and

$$T(\rho) = (s^{-1}G_s - G_{ss})_{s=\rho} - a^2\rho^{-2}(s^{-1}G_s - G_{ss})_{s=a} \tag{12}$$

4.2. Frictional Coefficient. For an infinitely long cylindrical volume C, eq 2 should be interpreted as an integral over a circular cross section cut perpendicular to the cylindrical axis. The resulting expression then gives the "force" per unit length on the infinite cylinder. This understood, the "force" functional is readily evaluated for the case when the cylinder axis is parallel to the z-axis. The velocity field is now given by $u = v_o u_{||}$ with $u_{||} = G(a)^{-1}G(a)(0,0,1)$. We find that the parallel component of the "force" functional $f_{||}$ and the frictional coefficient are given, respectively, by

$$f_{||} = 2\pi\Phi \tag{13a}$$

$$\xi_{||} = 2\pi\eta\Phi \tag{13b}$$

where the quantity $\Phi = (-sG^{-1}G_s)_{s=a}$.

When the axis of the cylinder is at right angles to the z-axis and thus to the fluid flow direction at large distance from the cylinder, we can express $f_\perp$ as

$$f_\perp = a\int[(2\cos^2(\varphi) + \sin(\varphi))(-r\partial_r u_{\perp x}) + \sin(\varphi)\cos(\varphi)(-r\partial_r u_{\perp y}) - \cos(\varphi)rP_\perp]_{|r=a}\,d\varphi \tag{14}$$

where we have used the fact that $T(a) = 0$. The function P appearing in eq 14 is the product $v_o P$, with $P_\perp = G(a)^{-1}a^2(s^{-1}G_s - G_{ss})_{s=a}z/r^2$. Noting that $(-rP_\perp)_{r=a} = \cos(\varphi)(2\Phi + a^2l^{-2})$ and $(-r\partial T)_{r=a} = -G(a)l^{-2}\Phi$, one can carry out the angle integral in eq 14 to find

$$f_\perp = \pi(4\Phi + a^2l^{-2}) \tag{15}$$

The corresponding frictional coefficient is

$$\xi_\perp = \pi\eta(4\Phi + a^2l^{-2}) \tag{16}$$

Observe that the "force" per unit length implied by eq 13a for the alignment of the cylinder parallel to the z-axis is equal to $2v_o\eta\pi\Phi$. Thus, the "force" per unit length on an infinite cylinder aligned parallel to the velocity field is less than half of the one aligned perpendicular to the velocity field.

5. Cylindrical Molecule of Finite Length

What is the friction on a cylindrical shaped molecule of finite length L moving through the gel with a constant velocity v_o? The variational approach described above enables us to estimate this number.

Let us recollect that the variational formulation assigns to a test function b with certain constraints, a positive number, whose

extremum allows us to calculate the "force" f_R. This extremum is achieved by the velocity field solution to the incompressible hydrodynamic equation.

Let f_L be the "force" from eq 4 on the length L cylinder averaged over the spherical angles that defines its orientation; let f_∞ denote the likewise averaged "force" per unit length on the infinite cylinder. Our basic result is that one can place upper and lower bounds on the "force"

$$f_\infty < L^{-1}f_L < [(1 + \alpha_1(l/L)^{1/2} + \alpha_2 l/L)f_\infty + (\alpha_3(l/L)^{1/2} + \alpha_4 l/L)\pi a^2/l^2] \quad (17)$$

The coefficients α_{1-4} depend only on the ratio l/L.

5.1. Lower Bounds on Force Functional. To obtain lower bounds on $f_{||,L}$, we let $\rho = (x^2 + y^2)^{1/2}$ and introduce the functional $H_{||}(b)$ on the test function b

$$H_{||}(b) = \iiint_{\{|z|\le L/2,\rho\ge a} (\partial_i b_j \partial b_j + l^{-2} b_i b_j) \quad (18)$$

with the constraint that it decays appropriately as $\rho \to \infty$ and equal (0,0,1) on the boundary $\rho = a$.

Observe that the velocity field $u_{||,\infty} = G(\rho)(0,0,1)$ that gives our solution to the infinite cylinder case is a critical point of $H_{||}$. Thus, $u_{||,\infty}$ minimizes $H_{||}$ and $H_{||}(u_{||,\infty}) = Rf_{||,\infty}$. Further, the length L solution $u_{||}$ is an allowable velocity field for $H_{||}$ and hence

$$Lf_{||,\infty} \le H_{||}(u_{||}) \quad (19)$$

The right-hand side of eq 19 is less than, where the volume Ω is the region outside the finite cylinder. But the integrand of this integral is not the same as eq 6 due to the presence of the term $\partial_i u_{||,j}\partial_j u_{||,i}$. One can show that this term makes vanishing contribution to the integral in eq 2 for $f_{||,L}$. Consequently, eq 19 implies the inequality

$$Lf_{||,\infty} < f_{||,L} \quad (20)$$

Next we consider the cylinder oriented along the x-axis and occupying the region where $|x| \le L/2$ and $r \equiv (z^2 + y^2)^{1/2} \le a$. We introduce the functional $H_\perp(b)$, which is of the same from as eq 6, except that the integration domain is restricted to points where $|x| \le L/2$. Arguments along the same line as before establish that there is a unique critical point of $H_\perp$ and that the value of $H_\perp$ at this critical point is its extremum over the allowed velocity field. The minimizer obeys eq 2 and $(\partial_x b_i + \partial_i b_x)$ vanishes on $|x| = L/2$; this is also the condition satisfied by $u_{\perp,\infty}$. Thus, $u_{\perp,\infty}$ is the minimizer of $H_\perp$ and $H_\perp(u_{\perp,\infty}) = Lf_{\perp\infty}$. Meanwhile, since the solution $u_\perp$ to the finite length cylinder is an allowable velocity field for $H_\perp$, we have $Lf_{\perp\infty} < H_\perp(u_\perp)$. This last inequality leads to the desired result

$$Lf_{\perp,\infty} < f_{\perp,L} \quad (21)$$

5.2. Upper Bounds on Force Functional. We now consider the case of determining an upper bound $f_{\perp,L}$. The strategy here is to first extend the velocity field $u_{\perp,\infty}$ to the region where $|x| \ge L/2$ and $r \equiv (z^2 + y^2)^{1/2} \le a$ as (0,0,1). What this does is to make the velocity field be defined over the outer region of the finite cylinder. Second, we introduce the function $\chi(x)$ along the cylindrical axis given by

$$\chi = \exp(-|x| + L/2)/l, -L/2 \le |x| \quad (22)$$

while it is unity for $|x| \le L/2$.

Observe that $b = \chi u_{\perp,\infty}$ is an allowable velocity field for the functional $\mathcal{F}$ so that $f_{\perp,L} \le \mathcal{F}(\chi u_{\perp,\infty})$, where

$$\mathcal{F}(\chi u_{\perp,\infty}) = (\int \chi^2\, dx) f_{\perp,\infty} + (\int dx\, \chi_x{}^2)\iint |u_{\perp,\infty}|^2 + l^2(\int_{|x|>L/2} \chi^2\, dx)\left(\iint_{\rho\le a} u_\perp{}^2\right) \quad (23)$$

The x-integrals can be carried out explicitly, and one obtains the desired inequality

$$f_{\perp,L} \le L[(1 + 2l/L)f_{\perp,\infty} + (1/L)2\pi a^2/l^2] \quad (24)$$

A similar analysis, though considerably more involved, leads to an upper bound for the "force" per unit length that acts parallel to the axis of the cylinder

$$f_{||,R} \le R(1 - X)^{-1}[(1 + AX + (1 + 2s + \beta)X^2)f_{||,\infty}, (BX + (1 + 2s)X^2)\pi a^2/l^2] \quad (25)$$

where $A = (1 + \pi/s + \pi^2/s^2)^2(3\beta + 2a^2/l^2)$, $B = (1 + \pi/s + \pi^2/s^2)^2\pi a^2/l^2(1 + a^2/l^2)$, $\beta = 2^{-1}(\Phi - \Phi^{-1}a^2/l^2)$, $X = (l/L)^{1/2}$, and the value of s is such that it minimizes eq 25 for fixed values of length and diameter of the finite cylinder.

6. Planar Bend

In this section, we illustrate the value of our variational approach by estimating the force on a bent cylinder oriented perpendicular to the applied electric field in terms of the bend angle and the force per unit length of a straight cylinder. As we presently lack tight analytic upper and lower bounds for a bent cylinder oriented at other angles to the applied field, we forego a discussion of such cases in this article.

The geometric set up of the bent cylinder is such that the straight cylinder is oriented with its axis perpendicular to the z-axis, i.e., along the x-axis and that the kink angle is in the $x-z$ plane. The boundary of the cylinder is the region defined by $|x| \le L/2$ and $(y^2 + z^2)^{1/2} = a$, $|x| = L/2$, and $(y^2 + z^2)^{1/2} \le a$. The kinked molecule, C_α, is described by an angle α whose values range from 0 to $\pi/2$; for $x \ge 0$ the axis of the cylinder extends to a distance $L/2$ along the line where $\cos(\alpha)z = -\sin(\alpha)x$, while for $x \le 0$ the axis extends a distance $L/2$ along the line where $\cos(\alpha)z = \sin(\alpha)x$.

Let us recollect that the "force" per unit length on a given cylinder is obtained by minimizing the function, $\mathcal{F}$, over test functions b with certain boundary conditions. Let v_α denote the minimizer of the C_α version of $\mathcal{F}$.

The basic idea for obtaining an upper bound for $f_{R,\alpha}$ is to use the solution $\hat{v}_o$ for the unkinked cylinder of length $L\cos(\alpha)$ to define a test function b that satisfies the required constraints. Observe that the velocity field v_α is symmetric with respect to the interchange of (x,y,z) to $(-x,y,z)$ and that this interchange preserves the boundary conditions. What this implies is that v_{ox} must vanish at $x = 0$.

The components of the test function b that satisfies the various constraints is

$$\begin{aligned} b_x(x,y,z) &= \cos(\alpha)\hat{v}_{ox}(x,y,z_\alpha) \\ b_y(x,y,z) &= \cos(\alpha)\hat{v}_{oy}(x,y,z_\alpha) \\ b_z(x,y,z) &= \hat{v}_{ox}(x,y,z_\alpha) - sign(x)\sin(\alpha)\hat{v}_{ox}(x,y,z_\alpha) \end{aligned} \quad (26)$$

where $z_\alpha = \cos(\alpha)z + \sin(\alpha)|x|$. The various integrals that appear in the "force" functional satisfy the inequality

$$\int_\Omega |b|^2 \le \cos(\alpha)^{-1}(1+2\sin(\alpha))\int_\Omega |\hat{v}_o|^2$$

$$\int_\Omega |\partial_y b|^2 \le \cos(\alpha)^{-1}(1+2\sin(\alpha))\int_\Omega |\partial_y \hat{v}_o|^2 \quad (27)$$

$$\int_\Omega |\partial_z b|^2 \le \cos(\alpha)(1+2\sin(\alpha))\int_\Omega |\partial_z \hat{v}_o|^2$$

with a corresponding expression for the integral of the square of the x-derivative of b. Substituting eq 27 into eq 6 and making use of the bounds on $f_{L,0}$ obtained in section 5 lead to the desired result

$$f_{L,\alpha} \le L(1+2\sin(\alpha))(1+\sin(\alpha))^2[(1+ 2\cos(\alpha)^{-1}l/L)f_{\perp,\infty} + \pi a^2/l^2] \quad (28)$$

A different and, for some purposes, better estimate for the upper bound for $f_{L,\alpha}$ is achieved by directly using the solution $v_{\perp,\infty}$ for the unkinked infinite cylindrical molecule, to construct the test function b for the case $\alpha \neq 0$ and the finite length cylinder problem

$$f_{L,\alpha} \le L(1+2\cos(\alpha)^{-1}l/L) \{f_{\perp,\infty} - 4^{-1}\sin(\alpha)^2(f_{\perp,\infty} + \pi a^2/l^2)\} + \cos(\alpha)^{-1}\pi a^2/l^2 \quad (29)$$

Similarly, we can estimate a lower bound for $f_{L,\alpha}$

$$f_{L,\alpha} \ge L(f_{\perp,\infty} - 2^{-1}\sin(\alpha)^2(f_{\perp,\infty} + \pi a^2/l^2)) \quad (30)$$

Thus, for small values of the bend angle α, the upper and the lower bounds given by eqs 29 and 30, respectively, are not too far apart. An implication of eq 30 is that the force on a cylinder with bend angle α (each arm makes angle α from the *z*-axis) and length L is no smaller than L times that of an infinite cylinder, oriented at an angle $\theta = \alpha$ with respect to the *z*-axis.

7. Application: Mobility of Intrinsically Curved DNA

The characteristics of a sequence directed intrinsic curvature of DNA have been investigated by diverse experimental techniques that range from gel electrophoretic mobilities[1−7] to hydroxyl radical footprinting.[14−16,18−25,36] A robust feature emerging from these investigations is that if 4−6 bp homopolymeric $(dA{\cdot}dT)_{4-6}$, i.e., A-tracts, are inserted so as to be in phase with the helical screw of B-DNA, then global curvature of the DNA double helix is observed.[14−16,18−20,26−32,36] Gel retardation studies of A-tracts by Crothers and co-workers and Thompson and Landy have demonstrated that oligomeric DNA with a bend at the center migrates slower than that of a bend of the same magnitude located near the ends of the molecule.[13,14,32]

A quantitative description of the gel electrophoretic mobility patterns of intrinsically curved DNA as yet has defied theoretical analysis. Two empirical relations are often used to describe the electrophoretic mobilities of intrinsically bent DNA molecules in gels. In the first approach, a quantity R_L is introduced and defined to be the ratio of the length of a size marker leading to the observed gel mobility, to the length of the multimer.[4,14,32] Thus, deviations of R_L from unity serve as a sensitive gauge of anomalous migration of curved fragments in gels. What is found from an analysis of the data is a relation between relative curvature and R_L first observed by Koo and Crothers:[4,14,32]

$$R_L = 1 + A(\text{relative..curvature})^2 \quad (31a)$$

In eq 31a, the number of A-tract molecules in one helical turn of DNA is identified with relative curvature,[14,32] while the quantity A is proportional to the square of the length of the multimer.[4] The parameters that define the junction model attribute the A-tract region as the source of global curvature; in contrast, the wedge model attributes the curvature to the writh of the flanking B-DNA regions. These models allow one to extract the absolute curvature of the curved sequences from eq 31a.[14−16,29−32]

In the second approach, the gel data are analyzed based on the reptation model. In the reptation model, the electrophoretic mobility is proportional to mean squared end-to-end distance of the molecule.[1−4] Thus, a curved DNA with a bend at the center would have a smaller end-to-end distance relative to a straight DNA, and consequently migrates slower than the straight DNA.[1−4] But there is a wealth of experimental data indicating that reptation cannot describe the electrophoretic mobility of ionic DNA oligomers less than approximately 600−800 bp.[18,37,43] The curved DNA molecules under experimental investigations are usually in the range of 120−300 bp.[14−16,18−20,26−32,36]

For quantitative purpose of extracting the bend angle from gel data, a calibration curve is usually constructed based on a semiempirical approach due to Thompson-Landy and Kerppola-Curran.[13,22,23,32] In the model, the ratio of the mobility of a DNA of length L, with a bend at its center, is compared with that of a straight DNA molecule of same length[13]

$$\mu_m = \mu_s \cos(\beta/2) \quad (31b)$$

Here, μ_m is the mobility of the DNA with a bend at its center, while μ_s is the corresponding mobility when the bend is at its end. The angle β in eq 31b is the "experimental" bend angle and is equal to π minus the angle at the bend between the two arms of the DNA molecule. Thus, our angle α is half of β. A weakness of this empirical relation is its inability to account for characteristics of the gel matrix, the ionic strength of the buffer, the interaction of the gel with DNA, and the polyelectrolyte features of DNA.[13]

On the basis of the variational approach developed in this work, we can predict the ratio of the mobility of a bend and a straight polyion, μ_m/μ_s. Suppose there is a bend occurring some distance L_1 from one end of DNA. Let $L_2 = L - L_1$ and let $\Delta = L_2 - L_1$. Each arm is bent to angle α from a straight configuration. Assume that the straight cylinder is aligned with angle θ to the *z*-axis. When L is large, most of the polyion knows nothing of the bent. Thus, from eqs 13 and 15, the force on the cylinder is nearly proportional to

$$L_1\left(1+\sin^2(\alpha+\theta)\left(1+\frac{a^2l^{-2}}{2\Phi}\right)\right) + L_2\left(1+\sin^2(\alpha-\theta)\left(1+\frac{a^2l^{-2}}{2\Phi}\right)\right) \quad (32)$$

The value for θ is obtained by minimizing the preceding; we find

$$\cos(2\theta) = \cos(2\alpha)/(\cos^2(2\alpha) + \sin^2(2\alpha)\Delta^2/L^2)^{1/2} \quad (33)$$

Substituting this value for θ into eq 32, one obtains the "force" from eq 4 as function of length of the polyion and the location of the bend from one end

$$f/L = 1 + \frac{1}{2}\left(1+\frac{a^2l^{-2}}{2\Phi}\right)(1-(\cos^2(2\alpha)+\sin^2(2\alpha)\Delta^2/L^2)^{1/2}) \quad (34)$$

In agreement with experimental data, eq 34 predicts that the

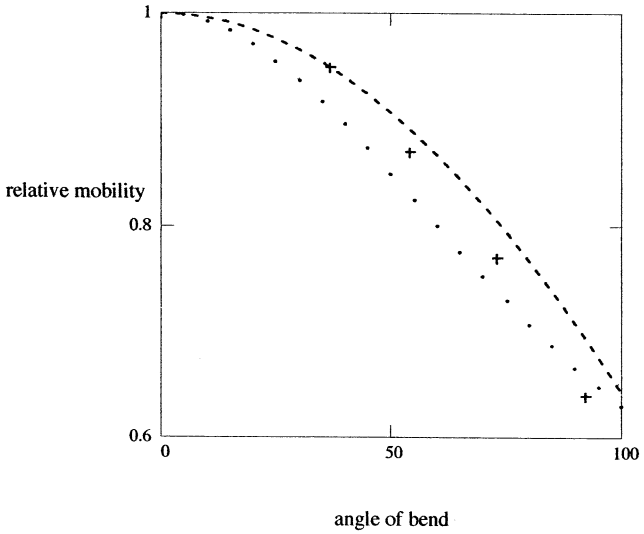

Figure 1. Plot of the relative mobility, i.e., the ratio of the gel electrophoretic mobility of a DNA molecule with a planar bend at the middle, with that of a straight DNA of the same length, vs the bend angle in degrees. The predictions of the model for a long DNA molecule (dotted line) are compared with the Thompson−Landy empirical relation for the mobility ratio (dashed line) and the experimental data (crosses) obtained from ref 13a. The diameter of the DNA is taken to be 20 Å, while the fiber spacing of the polyacrylamide gel has a prototypical value of 120 Å.

electrophoretic mobility of a polyion with a bend at the center is smaller than a bend located at some distance from the center. For the case that the bend is centrally located on the polyion, the mobility ratio is found to be

$$\mu_m/\mu_s = \frac{1}{1 + \sin^2(\beta/2)\left(1 + \frac{a^2 l^{-2}}{2\Phi}\right)} \qquad (35)$$

Here, β is twice the angle α that appears in the previous equations; we introduce it to compare our formula with that of Thompson−Landy in eq 31b. Note that by virtue of the appearance of l in eq 35, the mobility ratio depends on the hydrodynamic shielding length, a quantity that is a function of the viscosity of the solvent and the density of the gel fibers. Note also the dependence in eq 35 on the diameter of the polyion.

Figure 1 compares the predictions of our model given by eq 35 with the experimental data for oligomeric DNA, as well as the Thompson−Landy and Kerppola−Curran relation. We have taken the diameter of DNA to be that of B-DNA, namely, 20 Å. A prototypical value of 120 Å is taken to be fiber spacing of the gel. The parameters chosen are appropriate for DNA migrating in polyacrylamide gels. On solving the Bessel equation, one estimates that $\Phi \approx 4$. For small bend angles, our predictions agree with Thompson−Landy relation.

8. Discussion

Several comments are in order regarding our predictions based on eq 35. First, our conclusion that a bent rod has smaller mobility than a straight rod of the same length might be expected on the basis of the following considerations: As argued in section 4 and section 5 (see eqs 13a and 15, or 24 and 25), a very long rod oriented parallel to the applied electric field feels less than half the force per unit length of one of the same length, but aligned perpendicular to the electric field. This understood, a straight rod can then orient itself so that both arms are parallel to the applied electric field, but a bent rod must compromise. Thus, there is a larger force on the bent rod and so the bent rod has smaller mobility. This is the continuous density analogue of what is believed to occur when the gel is modeled by a lattice-like matrix of point sources of friction: A straight rod will slip through the rungs of the matrix while a bent one will get hung up.

TABLE 1: The Mobility Ratio as a Function of the Bend Angle for Prototypical Values of the Effective Diameter of DNA and the Hydrodynamic Shielding Length

angle of bend (deg)	50	70	90
mobility ratio			
(d = 50 Å; l = 120 Å)	0.846	0.748	0.662
(d = 50 Å; l = 80 Å)	0.842	0.743	0.656
mobility ratio			
(d = 100 Å; l =120 Å)	0.837	0.737	0.648
(d = 100 Å; l = 200 Å)	0.844	0.747	0.66

Second, eq 35 should be accurate to order $1/L$. Moreover, the order $(1/L)$ correction terms can be obtained using our variational formulation for the force functional with suitably chosen test functions. We expect that the computations of such correction terms will imporve the quantitative accuracy of what should be viewed as a first approximation.

Third, because the effective diameter of the polyion in our model is governed by the Debye screening length, Table 1 depicts the mobility ratio as a function of bend angle for prototypical values of the diameter and the hydrodynamic shielding length. Our results underscore the importance of the ratio of the diameter of the DNA molecule to the hydrodynamic shielding length in determining the characteristics of the mobility of bent and straight DNA.

Fourth, the effective charges of the straight polyion in free solution can be determined by counterion condensation formalism.[38] The effective charge of the planar bend DNA in free solution can be calculated by numerical counterion condensation along the lines formulated by Fenley et al.[39a] Since we are interested in mobility ratio of bent to straight DNA, we have assumed, as a first approximation, that the ratio of the effective charges in the two cases is near unity.[39a] In fact, for a weakly bend polyion, theoretical analysis corroborates this assumption (Odijk).[39b] An accurate calculation of the ratio of the effective charges could elucidate the small deviations from experimental data.

Fifth, another robust prediction that emerges from our estimate for the friction ratio of a long cylindrical molecule is that the dynamics of a cylindrically shaped molecule is such that the molecule will be oriented with high probability along the velocity field or equivalently along the external electric field. A verification of this prediction comes from linear dichroism (LD) spectroscopy study of DNA by Carlsson and Jonsson.[40] These authors investigated the electrophoretic migration of large DNA fragments in highly entangled polyacrylamide solution with molecular weight between 5×10^6 and 18×10^6.[40] The orientation factor S defined as[40]

$$S = (3\langle\cos^2\theta\rangle^{-1})/2 \qquad (36)$$

was obtained from the value of reduced dichroism $LD^r = LD/A_{iso}$, where the absorbency of an isotropic sample is denoted by A_{iso}. For random orientation of the molecules, $S = 0$, while for orientation parallel to the external field, $S = 1$. At voltages between 100 and 150 V/cm that is characteristic of capillary electrophoresis experiments, the average orientation of the DNA

is found to be $S \approx 0.7$.[40] Even in ultradilute polymer solutions, the DNA has an orientation factor of $S \approx 0.3$ at 100 V/cm.[40]

Limitations of the Model. In this section we provide an explanation for the fact that our equation in (3a) lacks an explicit electric field term. Indeed, such a term might be expected[35] to have a very complicated dependence on the DNA velocity, the gel matrix, the nature of the ionic species in the buffer, and the applied electric field. Our model is based on an assumption about the ultimate effect of these complicated ionic and electrical interactions. In particular, basic to our use of eq 3a is the assumption that during electrophoretic migration in the gel, the DNA experiences a net electric field that is, macroscopically, essentially constant in time and space.

To explain, note that the driving force due to the electric field will have the form qE, where q is an effective charge and E is the ambient electric field. However, our assumption of a constant electric field allows us to subsume this term into the constant velocity parameter v_o that appears in our definition of the unknown u. In fact, steady state considerations imply that v_0 can be expressed in terms of qE, the other parameters in eqs 3a, and whatever constant term is present in the gradient of the pressure. Note in this regard that the precise value of v_o does not enter our formulation since we are considering the ratio of the mobilities of bent and straight DNA.

Counterions from the bulk aqueous solution is expected to condense in a cloud around the DNA charges, thus partially screening the charges as predicted by counterion condensation and Poisson−Boltzmann models.[38,41] However, the calculations for the precise effect of the counterion cloud around a moving DNA molecule in a salt solutions are formidable, although one could, in principle, consider a perturbative expansion from the case with zero background electric field. In any event, we assume that this counterion cloud has but one electrophoretic effect and one hydrodynamic effect, these as described below. We postulate that this simplifying assumption is a reasonable approximation to the true state of affairs.

In our approximation, the sole effect of the counterion cloud on the electrophoretic properties of the DNA is to partially screen and thus effectively renormalize the charges along the DNA backbone. Thus, the counterions determine the effective charge q. Further, properties of the salt ions in the buffer enter our expression for the mobility ratio inasmuch as this ratio involves the cylinder diameter, a, and the viscosity of the solvent; both are determined by properties of the ions in the buffer. A method for computing this renormalized charge of DNA fragment approximately in gel has been proposed.[42]

For the purposes of hydrodynamic computations, the condensed ions and the Debye clouds decrease the mobility of the DNA molecule. In particular, it is an experimental fact[43−47] that the mobility of the DNA depends on the particulars of the salt ions in the buffer. As it is beyond our ability to compute the precise effects of the salt ions, we take the point of view that the surrounding counterion cloud makes for an effectively thicker DNA molecule which increases with decreasing ionic strength[48] and this increased thickness accounts for the decreased mobility. This manifests itself in our model through the choice for the diameter a of the DNA.

Finally, three comments are in order regarding our justification for the constant electric field assumption, and for our use of the parameters v_o and a to account for the effects of the buffer. First of all, the salt in the gel buffer is dissociated as a current flows through the gel during electrophoresis measurements. Second of all, the current is that predicted using the conductivity of the gel-free buffer.[49] Finally, the electric field in the gel can be measured and is observably constant at macroscopic scales.[50]

Acknowledgment. One of us (U.M.) thanks A. Spasic and N. Stellwagen for discussions. This work was supported by a grant (U.M.) from the National Science Foundation.

References and Notes

(1) Mohanty, U.; Searls, T.; McLaughlin, L. W. *J. Am. Chem. Soc.* **1998**, *120*, 8275−8276.
(2) Mohanty, U.; Searls, T.; McLaughlin, L. W. *J. Am. Chem. Soc.* **2000**, *122*, 1225−1226.
(3) Mohanty, U.; Searls, T.; McLaughlin, L. W. J. *Biomol. Struct. Dyn.* **2000**, *1*, 371−375.
(4) (a) Mohanty, U.; McLaughlin, L. W. *Annu. Rev. Phys. Chem*. **2001**, *52*, 93−106. (b) Mohanty, U.; McLaughlin, L. M. In *Physical Chemistry of Polyelectrolytes*; Radeva, T., Ed.; Marcel Dekker, Inc.: New York; pp 665−685.
(5) de Genne, P. G. *J. Chem. Phys.* **1972**, *55*, 572.
(6) Zimm, B. H.; Lumpkin, O. J. *Macromolecules* **1993**, *26*, 226.
(7) Lumpkin, O. J.; Levene S. D.; Zimm, B. H. *Phys. Rev. A* **1989**, *39*, 1573.
(8) Zimm, B. H. *J. Chem. Phys.* **1991**, *94*, 2187.
(9) Lumpkin, O. J.; Dejardin, P.; Zimm, B. H. *Biopolymers* **1985**, *24*, 1573.
(10) (a) Perkins, T. T.; Smith, D. E.; Chu, S. *Science* **1994**, *264*, 819. (b) Smith, D. E.; Perkins, T, T.; Chu, S. *Phys. Rev. Lett.* **1995**, *75*, 4146−4149.
(11) Levene, S. D.; Zimm, B. H. *Science* **1989**, *245*, 396.
(12) Zinkel, S. S.; Crothers, D. M. *Nature* **1987**, *328*, 178.
(13) (a) Thompson, J. F.; Landy, A. *Nuc. Acids Res.* **1988**, *16*, 9687. (b) Kerppola, T.; Curran, T. *Science* **1991**, *254*, 1210−1214.
(14) Koo, H.-S.; Crothers D. M. *Proc. Natl. Acad. Sci. U.S.A.* **1988**, *85*, 1763.
(15) Wu, H.-M.; Crothers, D. M. *Nature (London)* **1984**, *308*, 509.
(16) Koo, H.-S.; Crothers D. M. *Nature (London)* **1986**, *320*, 501.
(17) Zimm, B. H. *Curr. Opin. Struct. Biol.* **1993**, *3*, 373−376.
(18) (a) Calladine, C. R.; Drew, H. R.; McCall, M. J. *J. Mol. Biol.* **1988**, *201*, 127. (b) Calladine, C. R.; Collis, C. M.; Drew, H. R.; Mott, M. R. *J. Mol. Biol.* **1991**, *221*, 981.
(19) (a) Bolshoy, A.; McNamara, P.; Harrington, R. E.; Trifonov, E. N. *Proc. Natl. Acad. Sci. U.S.A.* **1991**, *88*, 2312. (b) Ulanovsky, L.; Trifonov, E. N. *Nature (London)* **1987**, *326*, 720.
(20) (a) Diekmann, S. *Nucl. Acids Res.* **1987**, *15*, 247. (b) Harrington, R. E. *Electrophoresis* **1993**, *14*, 732.
(21) Sitlani, A.; Crothers, D. M. *Proc. Natl. Acad. Sci. U.S.A.* **1998**, *95*, 1404−1409.
(22) Kerppola, T. K. *Proc. Natl. Acad. Sci. U.S.A.* **1996**, *93*, 10117.
(23) Kerppola, T. K.; Curran, T. *Science* **1991**, *254*, 1210−1214.
(24) (a) Kahn, J. D.; Crothers, D. M. *Cold Spring Harbor Symposium on Quantitative Biology*; Cold Spring Harbor Labortory Press: Cold Spring Harbor, NY, 1993; Vol. 54. (b) Kahn, J. D.; Crothers, D. M. *Proc. Natl. Acad. Sci. U.S.A.* **1992**, *89*, 6343.
(25) Burkhoff, A.; Tullis, T. D. *Cell* **1987**, *48*, 935.
(26) Crothers, D. M.; Haran, T. E.; Nadeau, J. G. *J. Biol. Chem.* **1990**, *265*, 7093.
(27) Milos, L.; Oslick, S.; Weiss, M. A. *J. Biol. Struct. Dyn.* **1997**, *14*, 911.
(28) (a) Young, M. A.; Beveridge, D. L. *J. Biol. Struct. Dyn.* **1997**, *14*, 824; see also Young, M. A.; Beveridge, D. L. Wesleyan University preprint, April **1998**. (b) Sprous, D.; Young, M. A.; Beveridge. D. L. *J. Biol. Struct. Dyn.* **1997**, *14*, 863.
(29) Ussery, D. W.; Bolshoy, A. *J. Biol. Struct. Dyn.* **1997**, *14*, 789.
(30) Trifonov, E. N. *Nuc. Acids Res.* **1980**, *8*, 4041.
(31) Trifonov, E. N. and Sussman, J. L. *Proc. Natl. Acad. Sci. U.S.A.* **1980**, *77*, 3816.
(32) (a) Koo, H. S. **1989**, Chapter 1, Ph.D. Thesis, Yale University. (b) Koo, H. S. Ph.D. Thesis, Chapter 2, Yale University, New Haven, CT 1989. (c) Koo, H. S. Thesis, Chapter 4, Yale University, New Haven, CT 1989.
(33) Stigter, D. *Macromolecules* **2000**, *33*, 8877−8889.
(34) Altenberger, A.; M. V. Tirrell, *J. Chem. Phys.* **1984**, *80*, 2208−2213.
(35) Tuebner, M. *J. Chem. Phys.* **1982**, *76*, 5564−5573.
(36) (a) Hagerman, P. J. *Nature (London)* **1986**, *321*, 449. (b) Hagerman, P. J. *Proc. Natl. Acad. Sci. U.S.A.* **1984**, *81*, 4632.
(37) Stellwagen, N. C. Private communication, 2002.
(38) Manning. G. S. *J. Phys. Chem.* **1981**, *85*, 1506−1515. (b) Manning, G. S. *Q. Rev. Biophys.* **1978**, *11*, 179.
(39) (a) Fenley M. O.; Manning, G. S.; Marky, N. L.; Olson, W. K. *Biophys Chem.* **1998** *74*, 135−52. (b) Odijk, T. *Physic A* **1991**, *176*, 201.

(40) Carlsson, C.; Jonsson, M. *Macromolecules* **1996**, *29*, 7802−7812.
(41) Ramanathan, G. V.; Woodbury, C. P., Jr. *J. Chem. Phys*. **1982**, *77*, 4133−4140.
(42) Stigter, D. *Biopolymers* **1992**, *31*, 169−176.
(43) Stellwagen, N. C. *Biochemistry* **1983**, *22*, 6−6193.
(44) (a) Stellwagen, N. C. *Electrophoresis* **1997**, *18*, 34−44. (b) Strutz, K.; Stellwagen, N. C. *Electrophoresis* **1998**, *19*, 635−642.
(45) Holmes, D. L.; Stellwagen, N. C. *Electrophoresis* **1991**, *12*, 253−263.
(46) Stellwagen, N. C.; Gelfi, C.; Righetti, G. P. *Biopolymers* **2000**, *54*, 137−142.
(47) Mohanty, U,; Stellwagen, N. C. *Biopolymers* **1998**, *49*, 209−214.
(48) (a) Stroobants, A.; Lekkerkerker, H. N. W.; Odijk, Th. *Macromolecules* **1986**, *19*, 2232−2238. (b) Nicolai, T.; Mandel, M. *Macromolecules* **1989**, *22*, 438−444.
(49) Stellwagen, N. C. Private communication, 2002.
(50) Houri, A.; Sudaka, P.; Geribaldi, S. M. *Appl. Theor. Electrophor*. **1991**, *1*, 323−331.